

5-22-2009

Experimental Studies of NaCs

Seth T. Ashman

Providence College, sashman@providence.edu

C. M. Wolfe

Lehigh University

J. P. Huennekens

Lehigh University

Follow this and additional works at: http://digitalcommons.providence.edu/physics_fac



Part of the [Atomic, Molecular and Optical Physics Commons](#)

Ashman, Seth T.; Wolfe, C. M.; and Huennekens, J. P., "Experimental Studies of NaCs" (2009). *Physics Faculty Publications*. 8.
http://digitalcommons.providence.edu/physics_fac/8

This Conference Proceeding is brought to you for free and open access by the Physics at DigitalCommons@Providence. It has been accepted for inclusion in Physics Faculty Publications by an authorized administrator of DigitalCommons@Providence. For more information, please contact mcaprio1@providence.edu.

Experimental Studies of NaCs

S. Ashman, C. M. Wolfe, J. Huennekens
Lehigh University, 16 Memorial Drive East, Bethlehem, PA 18015



Abstract

We present experimental studies of excited electronic states of the NaCs molecule that are currently underway in our laboratory. The optical-optical double resonance method is used to obtain Doppler-free excitation spectra for several excited states. These data are being used to obtain Rydberg-Klein-Rees (RKR) or Inverse Perturbation Approach (IPA) potential curves for these states. Bound-free spectra from single ro-vibrational levels of electronically excited states to the repulsive wall of the $1(a)\Sigma^+$ state are also being recorded. Using the previously determined excited state potentials, we can fit the repulsive wall of the $1(a)\Sigma^+$ state to reproduce the experimental spectra using LeRoy's BCNT program. A slightly modified version of BCNT will also be used to fit the relative transition dipole moments, $\mu_c(R)$, as a function of internuclear separation, R, for the various bound-free electronic transitions.

Why Study NaCs?

Large permanent dipole moment
Permanent Dipole Moments of Heteronuclear Alkali Molecules in $X^1\Sigma^+$ State

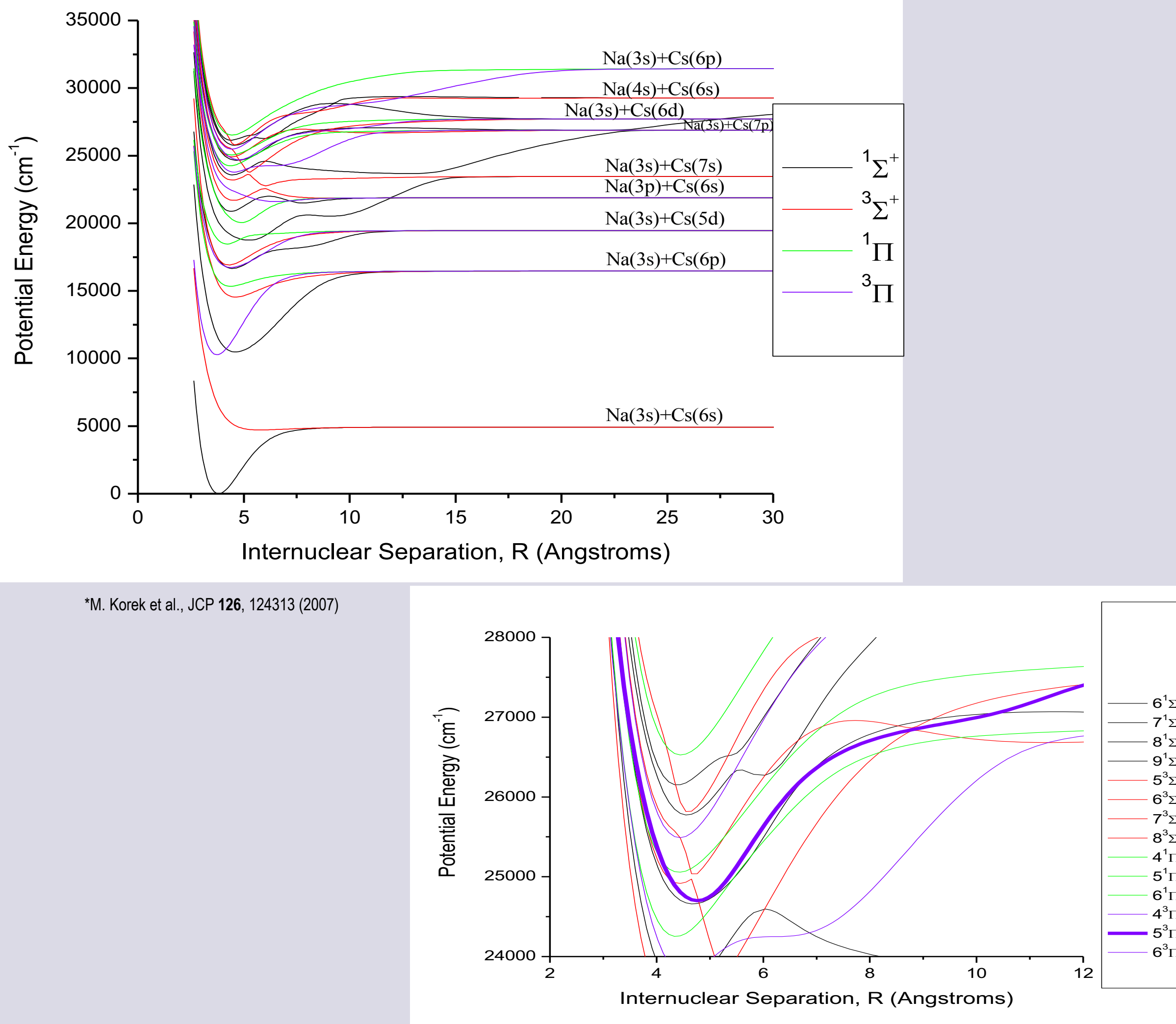
Molecule	Expt. Dipole(Dobye)
LiH	0.47
LiK	3.45
LiRb	4.05
LiCs	6.3
NaK	2.73
NaRb	4.72
NaCs	0.2
KRb	2.58
KCs	2.39
RbCs	2.39

Large spin-orbit interactions:

Spin-Orbit Splitting of Alkali Atoms ($E(P=3/2) - E(P=1/2)$)

Atomic symbol	Splitting (cm ⁻¹)
Li	0.335
Na	17.196
K	57.71
Rb	273.595
Cs	554.939
Fr	1696.599

NaCs Theoretical Potentials*



Goals

- Map excited state potentials
- Map repulsive wall of the $a^3\Sigma^+$ state
- Determine transition dipole moment functions, $\mu_c(R)$
- Study collisional energy transfer
- Measure spin-orbit coupling interaction parameters as functions of R
- Study hyperfine structure

Transition Dipole Moment and Selection Rules

Transition Dipole Moment Functions

Emission intensity for bound-bound or bound-free transitions is proportional to the square of the dipole matrix element

$$I_{\text{dipole}} = N_e \mu_a \mu_b \frac{8\pi^2}{3c\varepsilon_0} \frac{1}{R^3} |\mu_d|^2$$

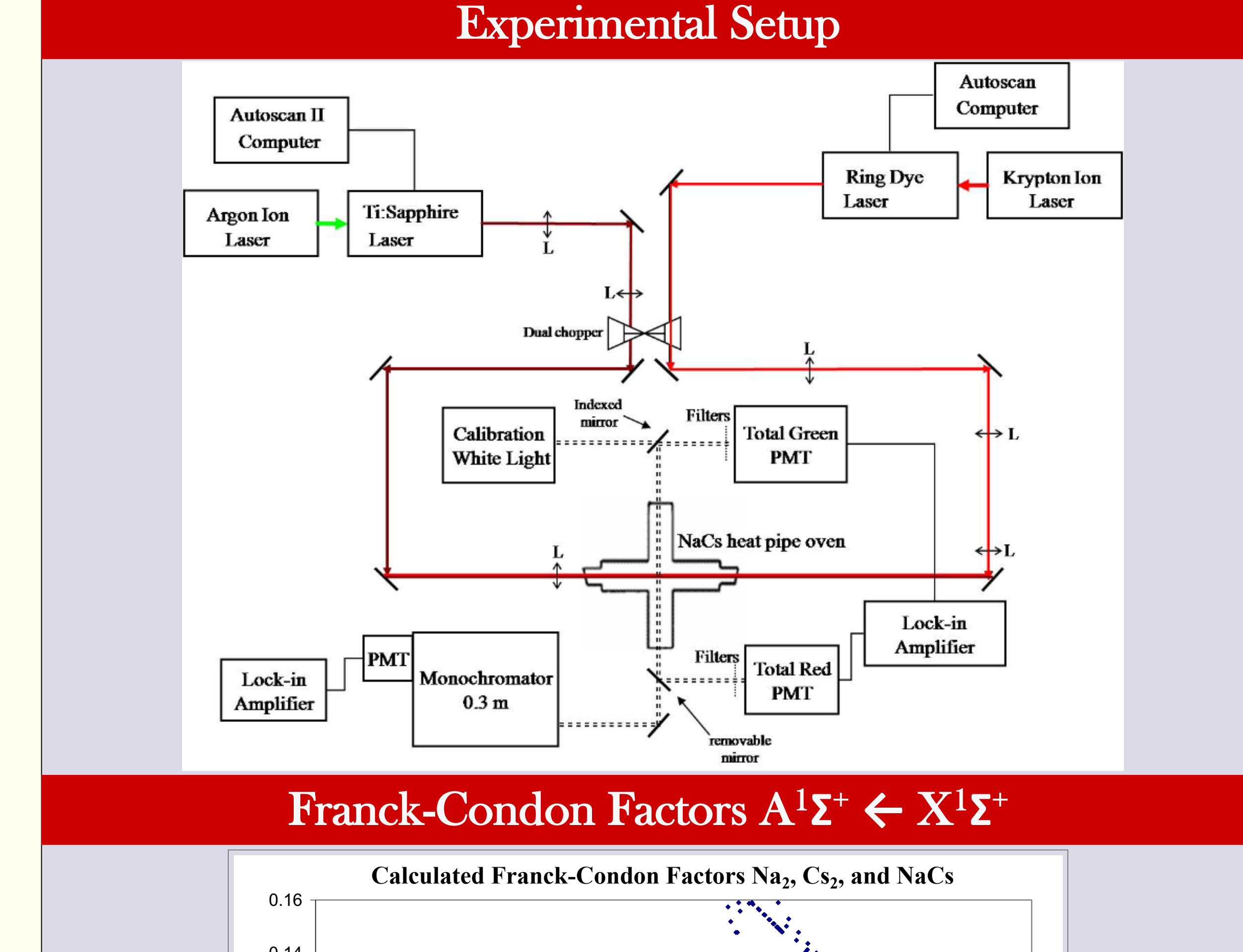
Here, $\mu_d = \int [Y_\ell^*(\vec{r}, R)] \Psi_a d\vec{r}_a \Psi_b^* d\vec{r}_b$, where $\mu_d = \mu_x + i\mu_y$ is the dipole operator

The total wave function can be separated into angular (rotational) and radial (vibrational) terms: $\Psi(\vec{r}, R) = \theta^\ell(\vec{r}, R) \psi^*(R) = \theta^\ell(\vec{r}, R) \frac{1}{R} \phi^\ell(R)$. Note that for bound-free transitions, the final state vibrational function must be replaced by a continuous function.

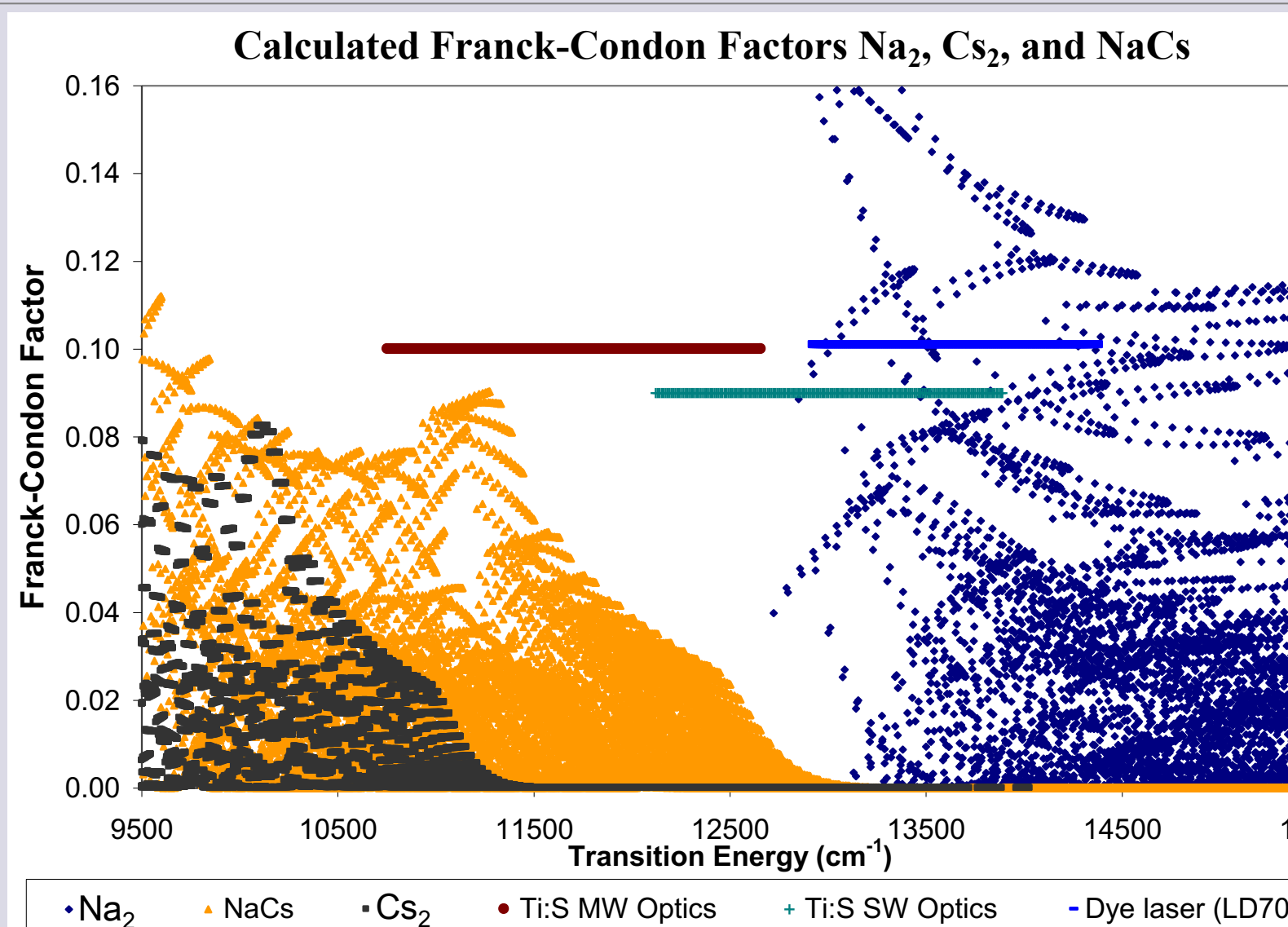
Thus the dipole matrix element becomes $\mu_d = \int [Y_\ell^*(\vec{r}, R)] (\psi^*)^2 (\partial_\ell + \partial_R) \Psi_a \Psi_b^* d\vec{r}_a d\vec{r}_b$. For a transition between two electronic states, initial state i and final state j , the selection term is zero, the angular terms of the μ_d integral lead to selection rules $\ell_i = \ell_j$ and the radial term leads to $\mu_d \propto \int x_i^{2\ell}(R) x_j^{2\ell}(R) dR$ with $\mu_d(R) = [\theta^\ell(\vec{r}, R) \partial_\ell \theta^\ell(\vec{r}, R)] dR$. Therefore, $\mu_d(R)$ can be obtained by fitting the intensities of bound-bound emission lines or bound-free emission counts to experimental spectra.

Selection Rules for Electronic Transitions

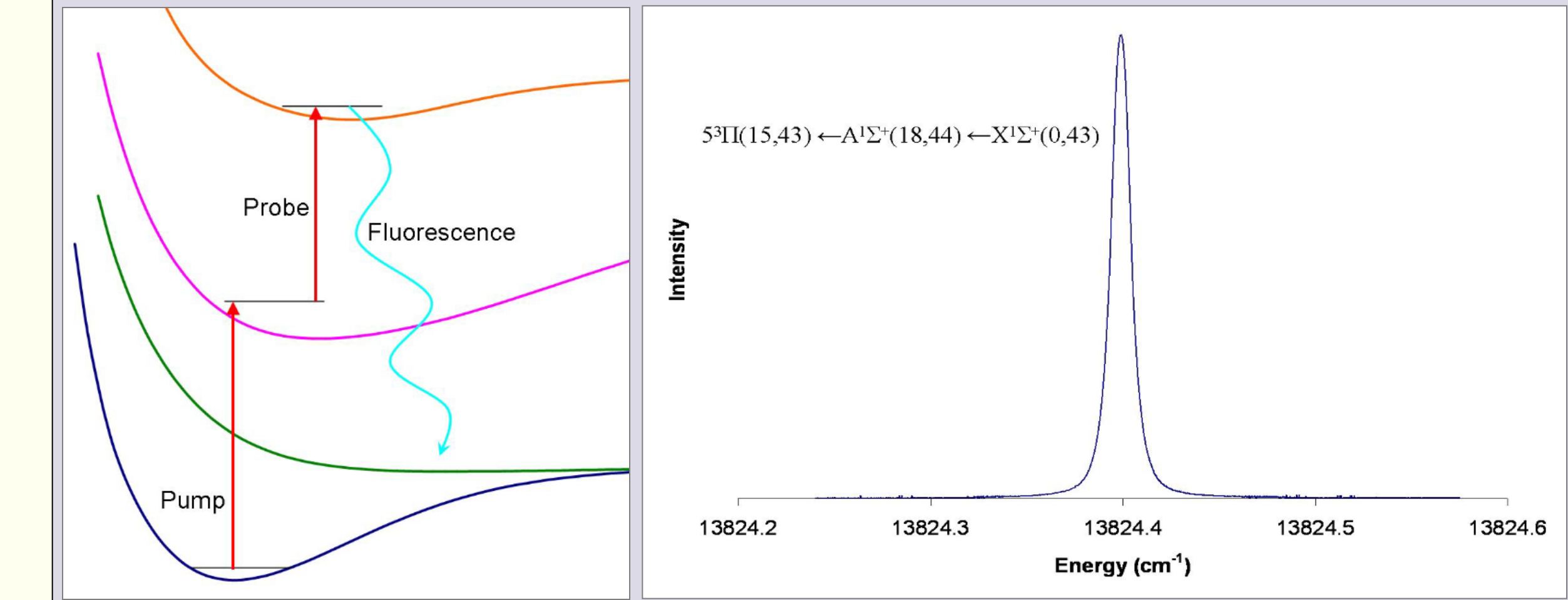
- Δv = anything
- $\Delta J = 0, \pm 1$ with restriction that $\Delta J = 0$ forbidden for $\Sigma \leftrightarrow \Sigma$ transitions
- Hund's case a)
 $\Delta S = 0$
 $\Delta \Lambda = 0, \pm 1$
 $\Delta \Omega = 0, \pm 1$
- Hund's case c)
 $\Delta \Omega = 0, \pm 1$



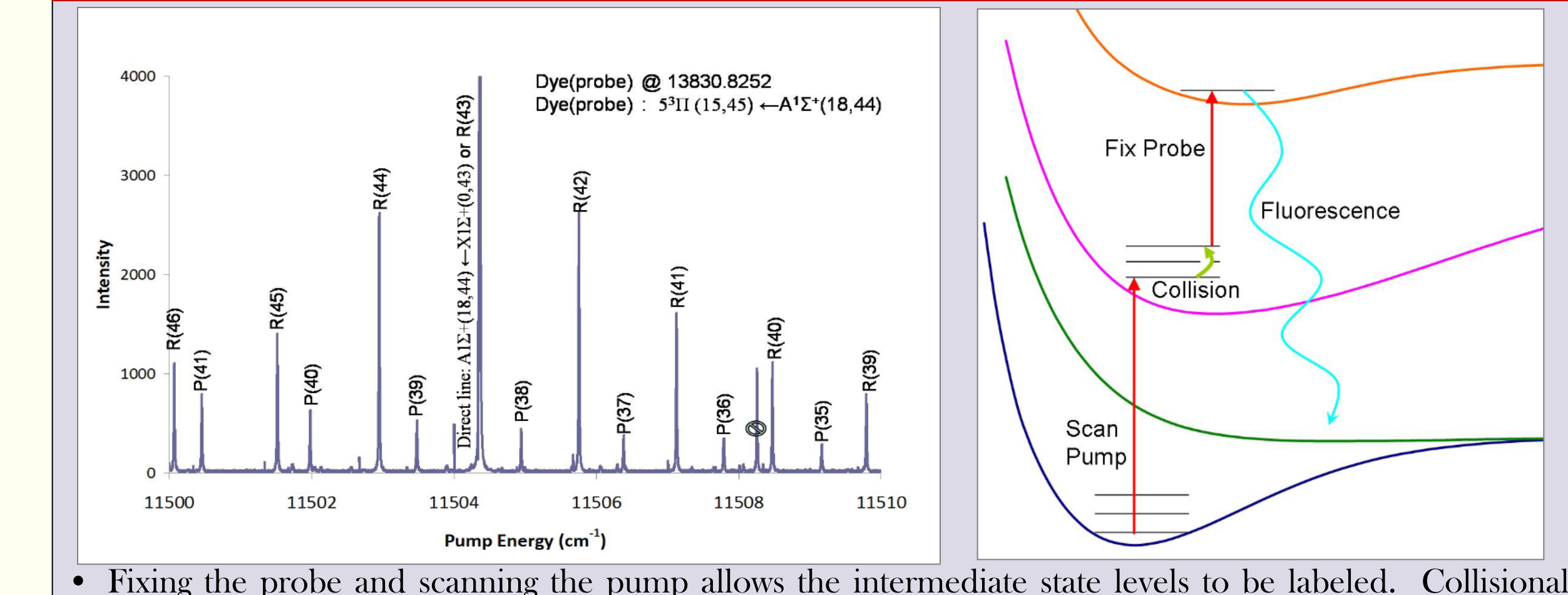
Franck-Condon Factors $A^1\Sigma^+ \leftarrow X^1\Sigma^+$



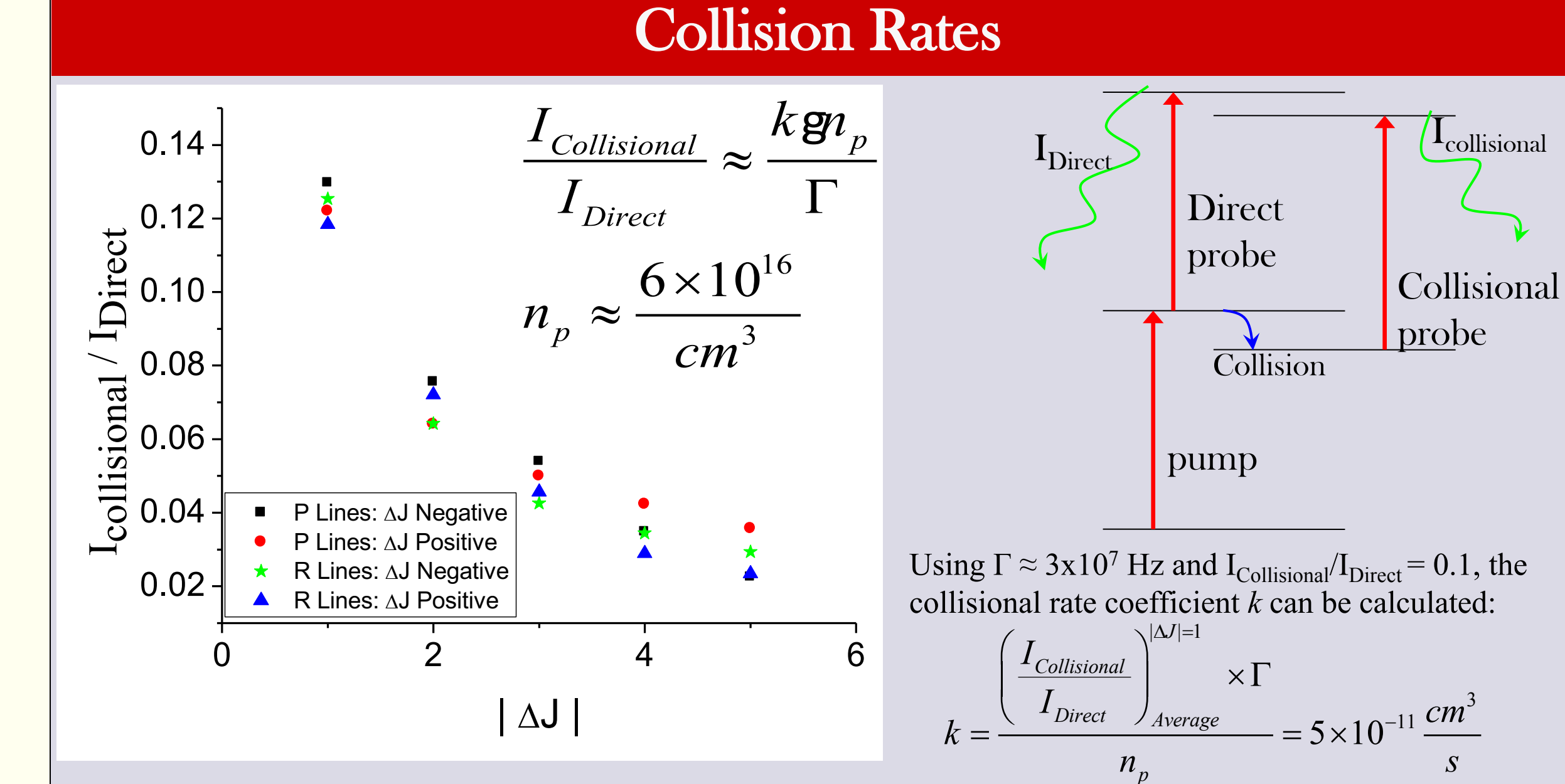
Double Resonance Excitation



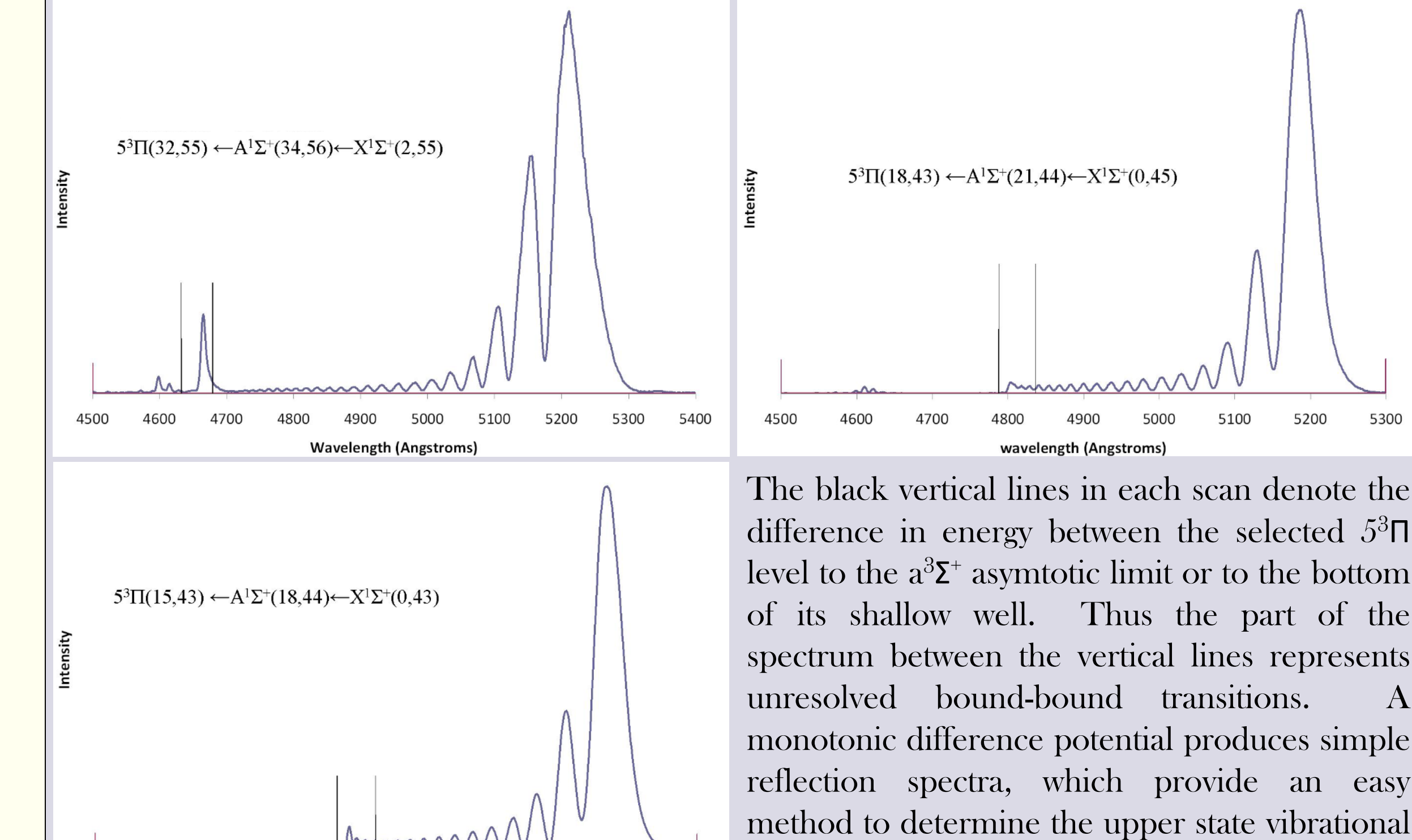
Collisional Population Transfer



- Fixing the probe and scanning the pump allows the intermediate state levels to be labeled. Collisional satellite lines allow intermediate state $[A^1\Sigma^+(v', J')]$ level energies for a large number of rotational levels to be determined relative to known ground state levels $[X^1\Sigma^+(v', J')]$.
- Then fixing the pump and scanning the probe allows the excited state levels to be labeled. Again collisional satellite lines allow the upper state level energies for a large number of rotational levels to be accurately determined relative to $A^1\Sigma^+(v', J')$ levels.

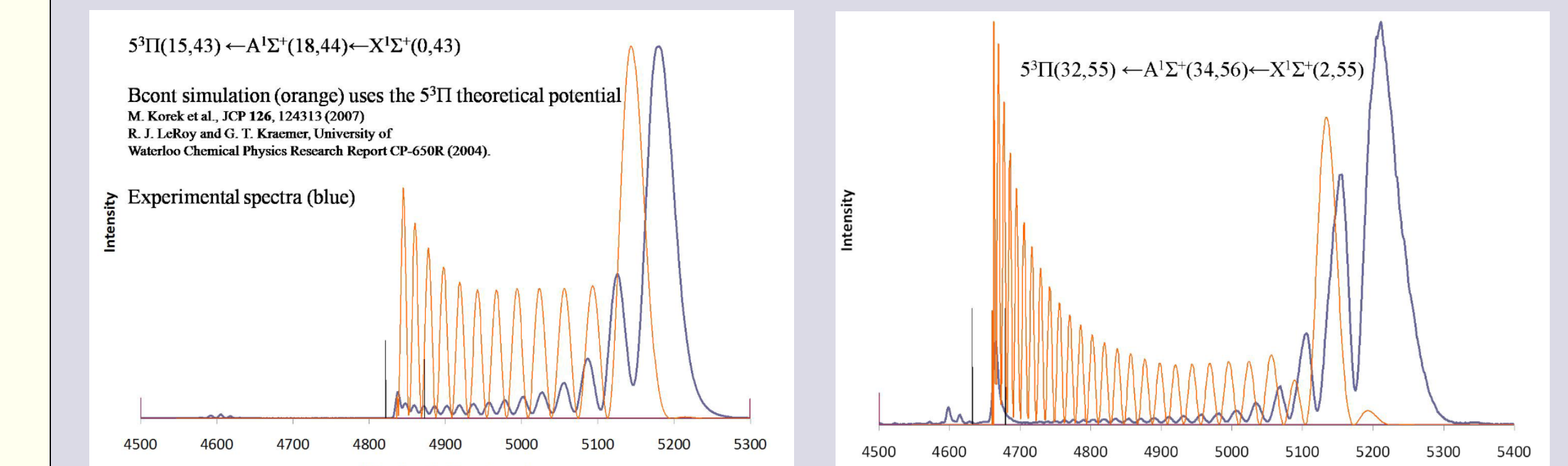


Resolved $5^3\Pi_0$ Fluorescence Spectra

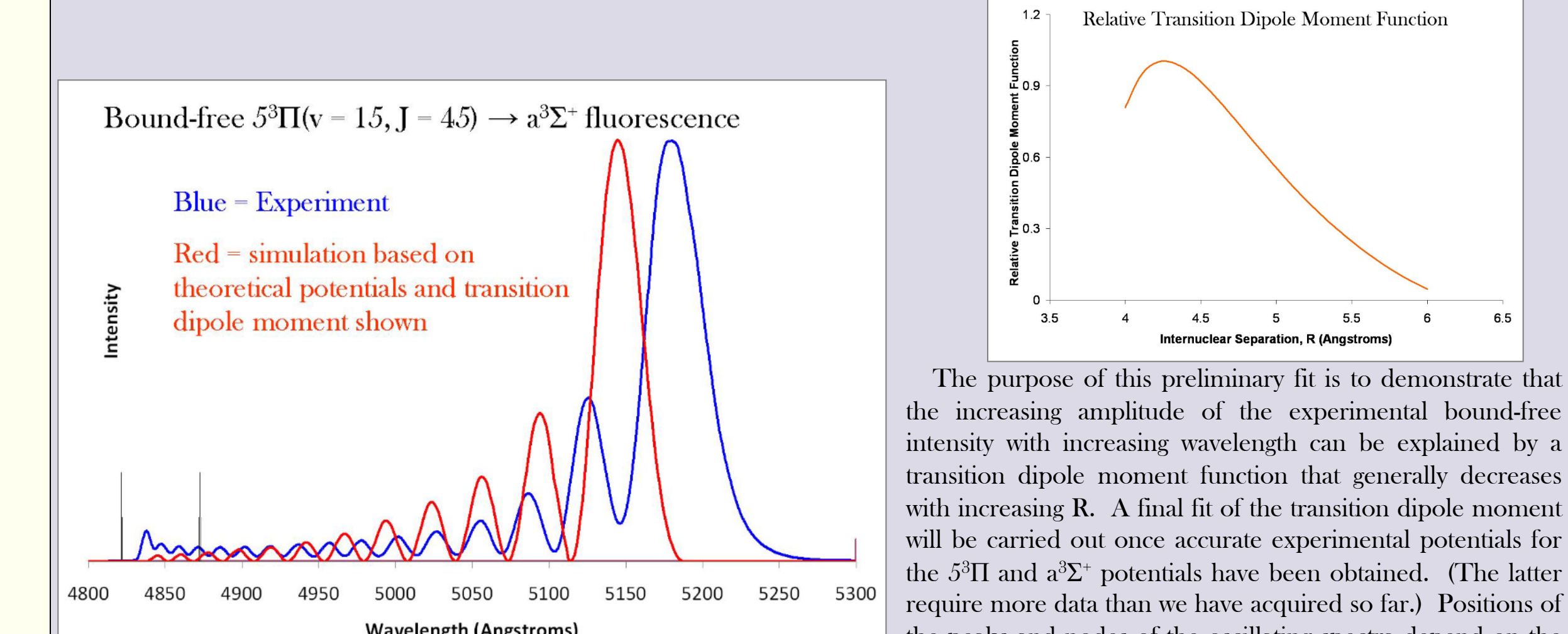


The black vertical lines in each scan denote the difference in energy between the selected $5^3\Pi$ level to the $a^3\Sigma^+$ asymptotic limit or to the bottom of its shallow well. Thus the part of the spectrum between the vertical lines represents unresolved bound-bound transitions. A monotonic difference potential produces simple reflection spectra, which provide an easy method to determine the upper state vibrational quantum number.

Spectra Simulation using BCNT: Constant Transition Dipole Moment



Spectra Simulation using BCNT: Fit of Relative Transition Dipole Moment Function

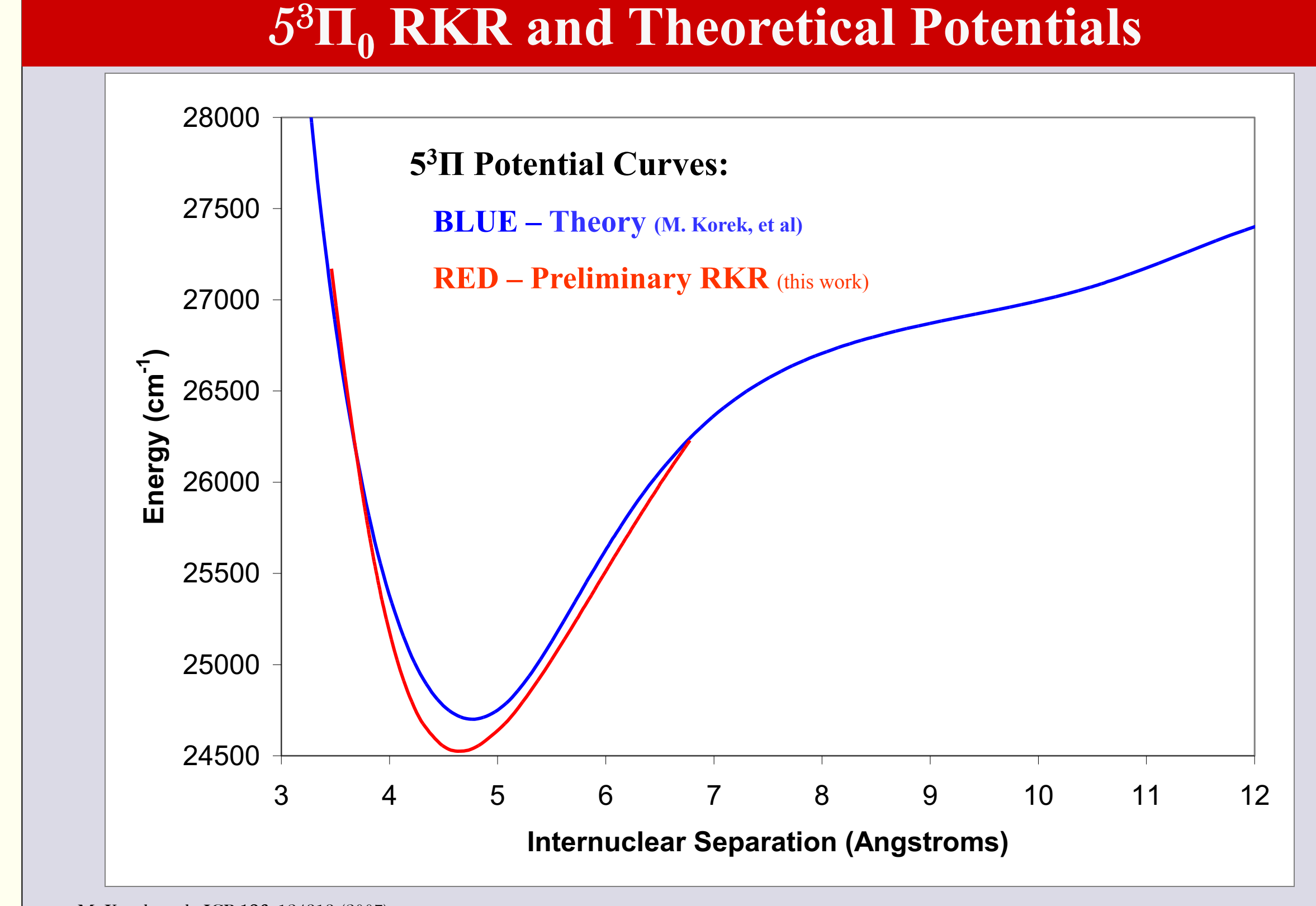


The purpose of this preliminary fit is to demonstrate that the increasing amplitude of the experimental bound-free intensity with increasing wavelength can be explained by a transition dipole moment function that generally decreases with increasing R. A final fit of the transition dipole moment will be carried out once accurate experimental potentials for the $5^3\Pi$ and $a^3\Sigma^+$ potentials have been obtained. (The latter require more data than we have acquired so far.) Positions of the peaks and nodes of the oscillating spectra depend on the upper and lower state potential energy curves while peak amplitudes depend on the transition dipole moment function.

Preliminary Dunham Coefficients for $5^3\Pi_0$ State

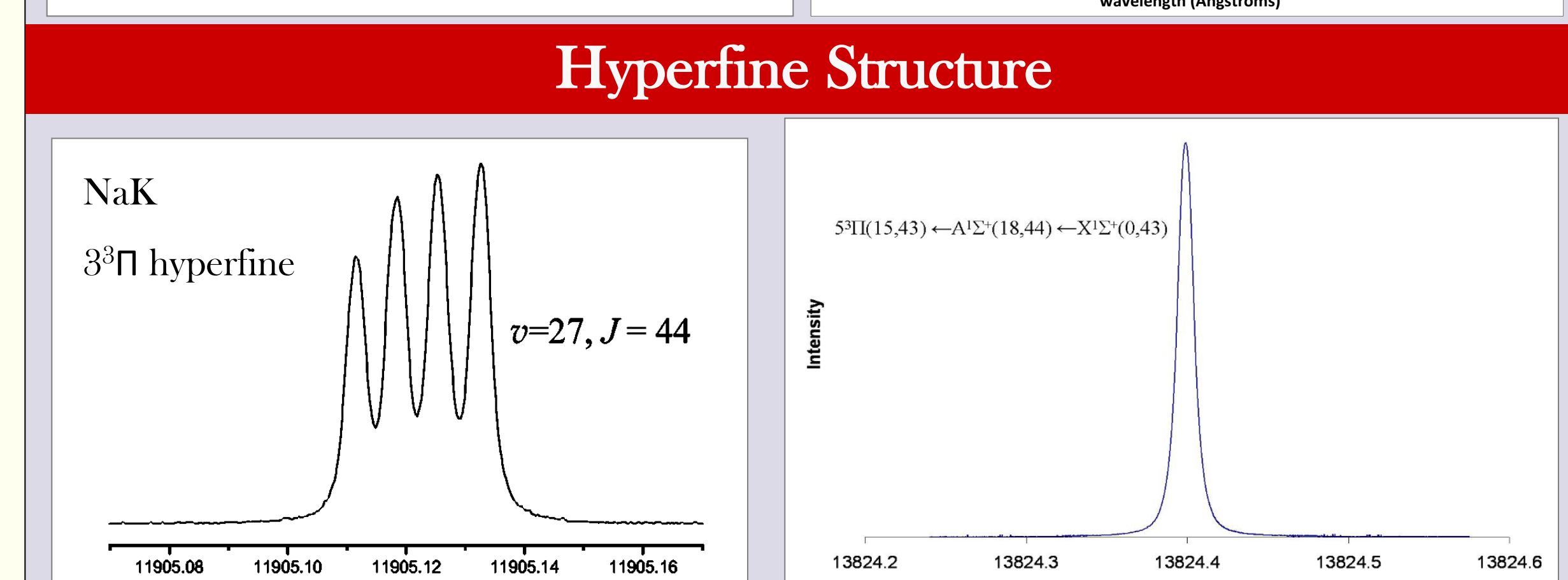
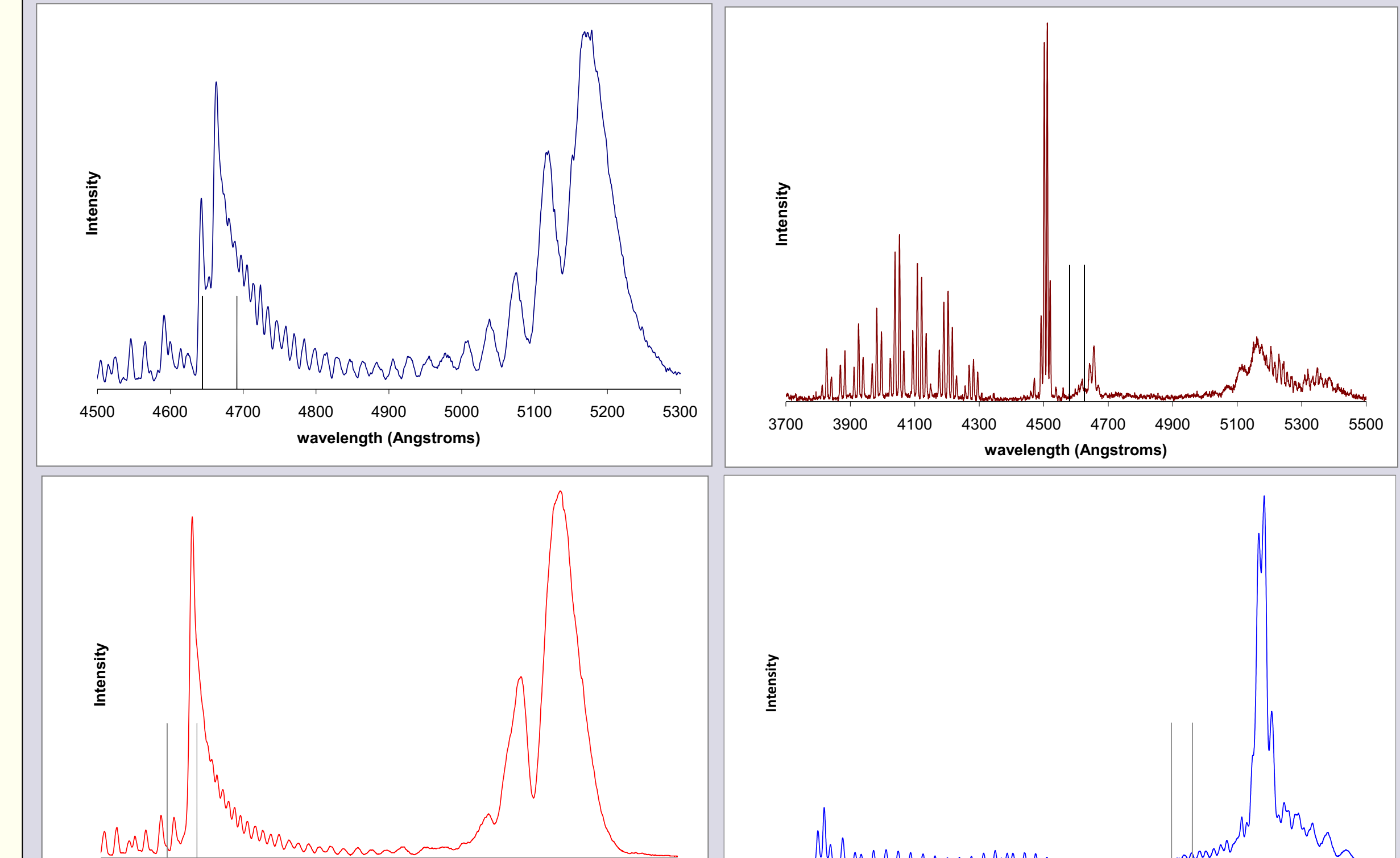
Parameter	Energy ± Error** (cm ⁻¹)	Theoretical values*** (cm ⁻¹)
T _e	24525.5 ± 6.2	24880
Y(1,0)	61.18 ± 0.55	58.6
Y(2,0)	-0.270 ± 0.013	-
Y(0,1)	0.0398 ± 0.0020	0.0394
Y(1,1)	(-2.4 ± 0.95) × 10 ⁻⁴	-
Y(0,2)	-2.0279 × 10 ⁻⁸ (fixed in fit)	-

*Fit using DPParfit program
R.J. LeRoy, DPParfit 3.3: A Computer Program for Fitting Multi-Isotopic Diatomic Molecular Spectra, University of Waterloo Chemical Physics Research Report CP-653 (2001)
**Statistical error only
***M. Kreck et al., JCP 126, 124313 (2007)



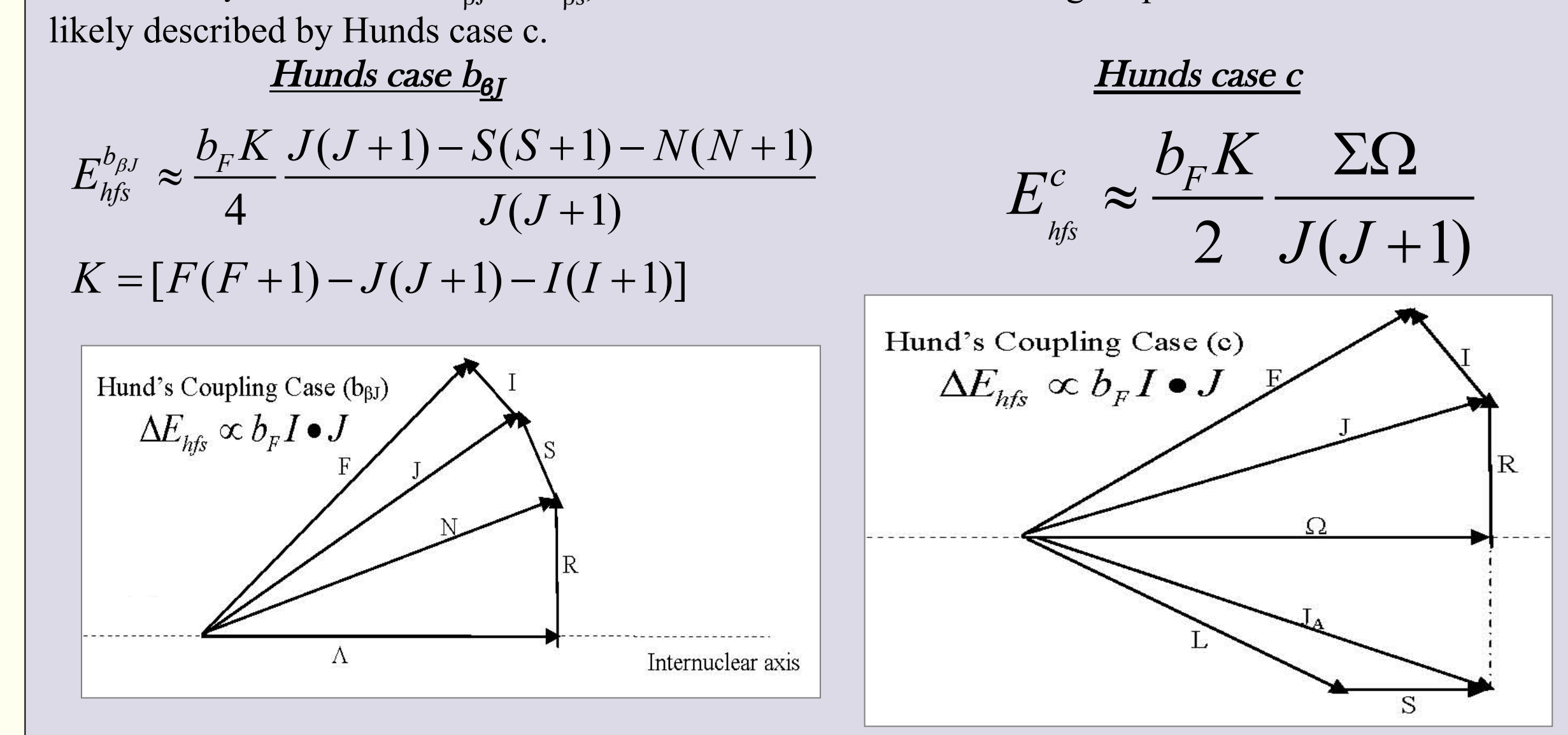
M. Kreck et al., JCP 126, 124313 (2007)
R.J. LeRoy, RKR 2.0: A Computer Program Implementing the First-Order RKR Method for Determining Diatomic Molecular Potential Energy Curves, University of Waterloo, Chemical Physics Research Report CP-657R (2004).

Spectra of Other NaCs Excited States Under Investigation



Previous work on NaK showed a rich variety of hyperfine structure. Ongoing studies of NaCs have yet to reveal clear hyperfine structure.
Hyperfine interaction in NaCs should be described by:
 $E_{hf} = b_F I \cdot S$
 $b_F^{Na} = 886 \text{ MHz}$ $I_{Na} = 3/2$
 $b_F^{Cs} = 2298 \text{ MHz}$ $I_{Cs} = 7/2$

From this we expect a larger hyperfine interaction for NaCs. However, states of NaK can often be described by Hund's case b_{hf} or b_{hf}^* , while NaCs has a much stronger spin-orbit interaction and is likely described by Hund's case c.



Therefore, the hyperfine structure might only be observable at lower J values than those we have studied.